

Movement Coordination

- 1 ARMIN FUCHS^{1,2}, J. A. SCOTT KELSO¹
 2 ¹ Center for Complex Systems & Brain Sciences,
 3 Florida Atlantic University, Boca Raton, USA
 4 ² Department of Physics, Florida Atlantic University,
 5 Boca Raton, USA

Article Outline

- 6 Glossary
 7 Definition of the Subject
 8 Introduction
 9 The Basic Law of Coordination: Relative Phase
 10 Stability: Perturbations and Fluctuations
 11 The Oscillator Level
 12 Breaking and Restoring Symmetries
 13 Conclusions
 14 Extensions of the HKB Model
 15 Future Directions
 16 Acknowledgment
 17 Bibliography

Glossary

- 18 **Control parameter** A parameter of internal or external
 19 origin that when manipulated controls the system
 20 in a nonspecific fashion and is capable of inducing
 21 changes in the system's behavior. These changes may
 22 be a smooth function of the control parameter, or
 23 abrupt at certain critical values. The latter, also referred
 24 to as phase transitions, are of main interest here as they
 25 only occur in nonlinear systems and are accompanied
 26 by phenomena like critical slowing down and fluctuation
 27 enhancement that can be probed for experimentally.
 28 **Haken–Kelso–Bunz (HKB) model** First published in
 29 1985, the HKB model is the best known and probably
 30 most extensively tested quantitative model in human
 31 movement behavior. In its original form it describes
 32 the dynamics of the relative phase between two oscillating
 33 fingers or limbs under frequency scaling. The HKB model
 34 can be derived from coupled nonlinear oscillators and has
 35 been successfully extended in various ways, for instance,
 36 to situations where different limbs like an arm and a leg,
 37 a single limb and a metronome, or even two different
 38 people are involved.
 39 **Order parameter** Order parameters are quantities that
 40 allow for a usually low-dimensional description of the
 41 dynamical behavior of a high-dimensional system on a
 42 macroscopic level. These quantities change their val-

ues abruptly when a system undergoes a phase transition. For example, density is an order parameter in the ice to water, or water to vapor transitions. In movement coordination the most-studied order parameter is relative phase, i. e. the difference in the phases between two or more oscillating entities.

Phase transition The best-known phase transitions are the changes from a solid to a fluid phase like ice to water, or from fluid to gas like water to vapor. These transitions are called first-order phase transitions as they involve latent heat, which means that a certain amount of energy has to be put into the system at the transition point that does not cause an increase in temperature. For the second-order phase transitions there is no latent heat involved. An example from physics is heating a magnet above its Curie temperature at which point it switches from a magnetic to a nonmagnetic state. The qualitative changes that are observed in many nonlinear dynamical systems when a parameter exceeds a certain threshold are also such second-order phase transitions.

Definition of the Subject

Movement Coordination is present all the time in daily life but tends to be taken for granted when it works. One might say it is quite an **archaic** subject also for science. This changes drastically when some pieces of the locomotor system are not functioning properly because of injury, disease or age. In most cases it is only then that people become aware of the complex mechanisms that must be in place to control and coordinate the hundreds of muscles and joints in the body of humans or animals to allow for maintaining balance while maneuvering through rough terrains, for example. No robot performance comes even close in such a task.

Although these issues have been around for a long time it was only during the last quarter century that scientists developed quantitative models for movement coordination based on the theory of nonlinear dynamical systems. Coordination dynamics, as the field is now called, has become arguably the most developed and best tested quantitative theory in the life sciences.

More importantly, even though this theory was originally developed for modeling of bimanual finger movements, it has turned out to be universal in the sense that it is also valid to describe the coordination patterns observed between different limbs, like an arm and a leg, different joints within a single limb, like the wrist and elbow, and even between different people that perform movements while watching each other.

Please note that the pagination is not final; in the print version an entry will in general not start on a new page.

95 Introduction

96 According to a dictionary definition: *Coordination* is the
97 act of coordinating, making different people or things
98 work together for a goal or effect.

99 When we think about *movement coordination* the
100 “things” we make work together can be quite different like
101 our legs for walking, fingers for playing the piano, mouth,
102 tongue and lips for articulating speech, body expressions
103 and the interplay between bodies in dancing and ballet,
104 tactics and timing between players in team sports and so
105 on, not to forget other advanced skill activities like skiing
106 or golfing.

107 All these actions have one thing in common: they look
108 extremely easy if performed by people who have learned
109 and practiced these skills, and they are incredibly difficult
110 for novices and beginners. Slight differences might exist
111 regarding how these difficulties are perceived, for instance
112 when asked whether they can play golf some people may
113 say: “I don’t know, let me try”, and they expect to out-drive
114 Tiger Woods right away; there are very few individuals
115 with a similar attitude toward playing the piano.

116 The physics of golf as far as the ball and the club is
117 concerned is almost trivial: hit the ball with the highest
118 possible velocity with the club face square at impact, and
119 it will go straight and far. The more tricky question is
120 how to achieve this goal with a body that consists of hun-
121 dreds of different muscles, tendons and joints, and, im-
122 portantly, their sensory support in joint, skin and muscle
123 **support** (proprioception), in short, hundreds of degrees
124 of freedom. How do these individual elements work to-
125 gether, how are they coordinated? Notice, the question is
126 not how do *we* coordinate them? None of the skills men-
127 tioned above can be performed by consciously controlling
128 all the body parts involved. Conscious thinking sometimes
129 seems to do more harm than good. So how do they/*we*
130 do it? For some time many scientists sought the answer to
131 this question in what is called *motor programs* or, more re-
132 cently, *internal models*. The basic idea is straightforward:
133 when a skill is learned it is somehow stored in the brain
134 like a program in a computer and simply can be called
135 and executed when needed. Additional learning or train-
136 ing leads to skill improvement, interpreted as refinements
137 in the program. As intuitive as this sounds and even if one
138 simply ignores all the unresolved issues like how such pro-
139 grams gain the necessary flexibility or in what form they
140 might be stored in the first place, there are even deeper rea-
141 sons and arguments suggesting that humans (or animals
142 for that matter) don’t work like that. One of the most strik-
143 ing of these arguments is known as motor equivalence: ev-
144 erybody who has learned to write with one of their hands

145 can immediately write with the foot as well. This writing
146 may not look too neat, but it will certainly be readable
147 and represents the transfer of a quite complex and diffi-
148 cult movement from one end-effector (the hand) to an-
149 other (the foot) that is controlled by a completely different
150 set of muscles and joints. Different degrees of freedom and
151 redundancy in the joints can still produce the same output
152 (the letters) immediately, i. e. without any practice.

153 For the study of movement coordination a most im-
154 portant entry point is to look at situations where the move-
155 ment or coordination pattern changes abruptly. An exam-
156 ple might be the well-known gait switches from walk to
157 trot to gallop that horses perform. It turns out, however,
158 that switching among patterns of coordination is a ubiq-
159 uitous phenomenon in human limb movements. As will
160 be described in detail, such switching has been used to
161 probe human movement coordination in quantitative ex-
162 periments.

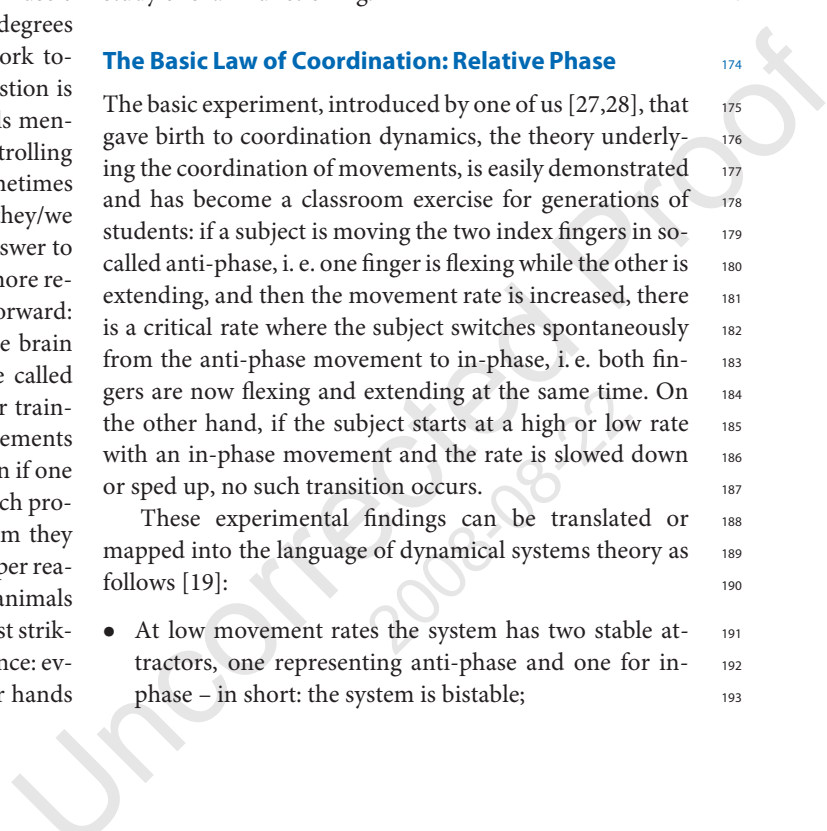
163 It is the aim of this article to describe an approach to
164 a quantitative modeling of human movements, called co-
165 ordination dynamics, that deals with quantities that are ac-
166 cessible from experiments and makes predictions that can
167 and have been tested. The intent is to show that coordi-
168 nation dynamics represents a theory allowing for quanti-
169 tative predictions of phenomena in a way that is unprece-
170 dented in the life sciences. In parallel with the rapid de-
171 velopment of noninvasive brain imaging techniques, co-
172 ordination dynamics has even pointed to new ways for the
173 study of brain functioning.

The Basic Law of Coordination: Relative Phase 174

175 The basic experiment, introduced by one of us [27,28], that
176 gave birth to coordination dynamics, the theory underly-
177 ing the coordination of movements, is easily demonstrated
178 and has become a classroom exercise for generations of
179 students: if a subject is moving the two index fingers in so-
180 called anti-phase, i. e. one finger is flexing while the other is
181 extending, and then the movement rate is increased, there
182 is a critical rate where the subject switches spontaneously
183 from the anti-phase movement to in-phase, i. e. both fin-
184 gers are now flexing and extending at the same time. On
185 the other hand, if the subject starts at a high or low rate
186 with an in-phase movement and the rate is slowed down
187 or sped up, no such transition occurs.

188 These experimental findings can be translated or
189 mapped into the language of dynamical systems theory as
190 follows [19]:

- 191 • At low movement rates the system has two stable at-
192 tractors, one representing anti-phase and one for in-
193 phase – in short: the system is bistable;



- 194 • When the movement rate reaches a critical value, the
195 anti-phase attractor disappears and the only possible
196 stable movement pattern remaining is in-phase;
- 197 • There is strong hysteresis: when the system is perform-
198 ing in-phase and the movement rate is decreased from
199 a high value, the anti-phase attractor may reappear but
200 the system does not switch to it.

201 In order to make use of dynamical systems theory for
202 a quantitative description of the transitions in coordinated
203 movements, one needs to establish a measure that allows
204 for a formulation of a dynamical system that captures
205 these experimental observations and can serve as a phe-
206 nomenological model. Essentially, the finger movements
207 represent oscillations (as will be discussed in more detail
208 in Subsect. “Oscillators for Limb Movements”) each of
209 which is described by an amplitude r and a phase $\varphi(t)$. For
210 the easiest case of harmonic oscillations the amplitude r
211 does not depend on time and the phase increases linearly
212 with time at a constant rate ω , called the angular velocity,
213 leading to $\varphi(t) = \omega t$. Two oscillators are said to be
214 in the in-phase mode if the two phases are the same, or
215 $\varphi_1(t) - \varphi_2(t) = 0$, and in anti-phase if the difference between
216 their two phases is 180° or π radians. Therefore, the
217 quantity that is most commonly used to model the exper-
218 imental findings in movement coordination is the phase
219 difference or *relative phase*

$$\phi(t) = \varphi_1(t) - \varphi_2(t) = \begin{cases} \phi(t) = 0 & \text{for in-phase} \\ \phi(t) = \pi & \text{for anti-phase} \end{cases} \quad (1)$$

221 The minimal dynamical system for the relative phase
222 that is consistent with observations is known as the
223 Haken–Kelso–Bunz (or HKB) model and was first pub-
224 lished in a seminal paper in 1985 [19]

$$\dot{\phi} = -a \sin \phi - 2b \sin 2\phi \quad \text{with} \quad a, b \geq 0. \quad (2)$$

226 As is the case for all one-dimensional first order differen-
227 tial equations, (2) can be derived from a potential function

$$\dot{\phi} = -\frac{dV(\phi)}{d\phi} \quad \text{with} \quad V(\phi) = -a \cos \phi - b \cos 2\phi. \quad (3)$$

229 One of the two parameters a and b that appear in (2)
230 and (3) can be eliminated by introducing a new time scale
231 $\tau = \alpha t$, a procedure known as scaling and commonly used
232 within the theory of nonlinear differential equations, lead-

ing to

$$\begin{aligned} \dot{\phi}(t) &= \frac{d\phi(t)}{dt} \rightarrow \frac{d\phi\left(\frac{\tau}{\alpha}\right)}{d\frac{\tau}{\alpha}} \\ &= -a \sin \phi\left(\frac{\tau}{\alpha}\right) - 2b \sin 2\phi\left(\frac{\tau}{\alpha}\right) \quad (4) \\ \alpha \frac{d\tilde{\phi}(\tau)}{d\tau} &= -a \sin \tilde{\phi}(\tau) - 2b \sin 2\tilde{\phi}(\tau) \end{aligned}$$

where $\tilde{\phi}$ has the same shape as ϕ , it is just changing on
a slower or faster time scale depending on whether α is
bigger or smaller than 1. After dividing by α and letting
the so far undetermined $\alpha = a$ (4) becomes

$$\frac{d\tilde{\phi}}{d\tau} = -\underbrace{\frac{a}{\alpha}}_{=1} \sin \tilde{\phi} - 2 \underbrace{\frac{b}{\alpha}}_{=k} \sin 2\tilde{\phi}. \quad (5)$$

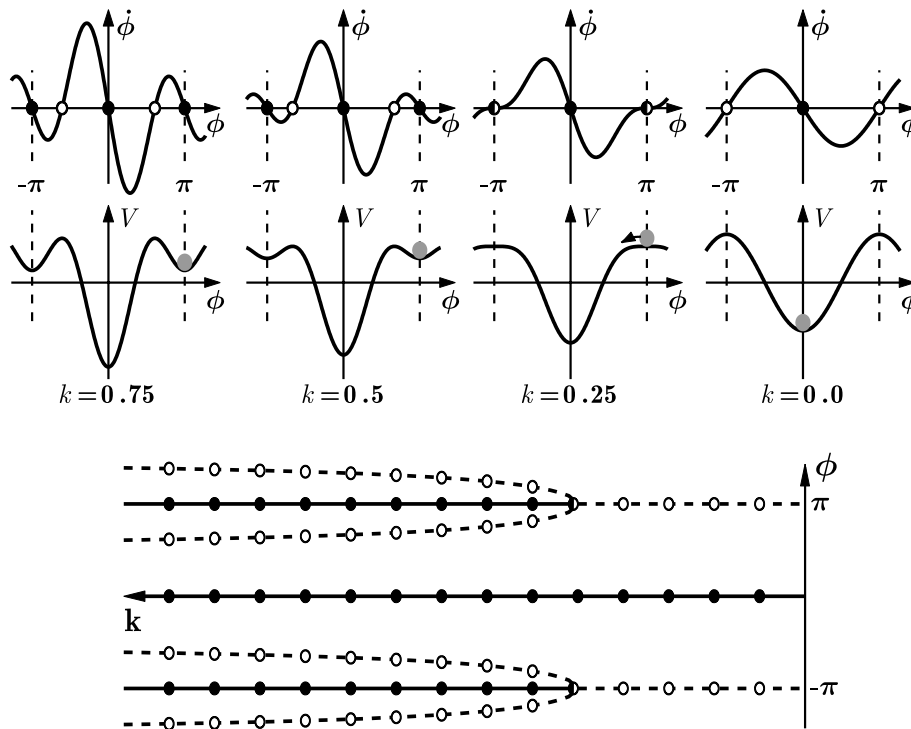
Finally, by dropping the tilde (2) and (3) can be written
with only one parameter $k = \frac{b}{a}$ in the form

$$\begin{aligned} \dot{\phi} &= -\sin \phi - 2k \sin 2\phi \\ &= -\frac{dV(\phi)}{d\phi} \quad \text{with} \quad V(\phi) = -\cos \phi - k \cos 2\phi. \quad (6) \end{aligned}$$

The dynamical properties of the HKB model’s *collective*
or *coordinative* level of description are visualized in
Fig. 1 with plots of the phase space ($\dot{\phi}$ as a function of ϕ)
in the top row, the potential landscapes $V(\phi)$ in the second
row and the bifurcation diagram at the bottom. The control
parameter k , as shown, is the ratio between b and a ,
 $k = \frac{b}{a}$, which is inversely related to the movement rate:
a large value of k corresponds to a slow rate, whereas k
close to zero indicates that the movement rate is high.

In the phase space plots (Fig. 1 top row) for $k = 0.75$
and $k = 0.5$ there exist two stable fixed points at $\phi = 0$
and $\phi = \pi$ where the function crosses the horizontal axis
with a negative slope, marked by solid circles (the fixed
point at $-\pi$ is the same as the point at π as the function is
 2π -periodic). These attractors are separated by repellers,
zero crossings with a positive slope and marked by open
circles. For the movement rates corresponding to these
two values of k the model suggests that both anti-phase
and in-phase movements are stable. When the rate is in-
creased, corresponding to a decrease in the control param-
eter k down to the critical point at $k_c = 0.25$ the former
stable fixed point at $\phi = \pi$ collides with the unstable fixed
point and becomes neutrally stable indicated by a half-
filled circle. Beyond k_c , i. e. for faster rates and smaller val-
ues of k the anti-phase movement is unstable and the only
remaining stable coordination pattern is in-phase.

The potential functions, shown in the second row in
Fig. 1, contain the same information as the phase space



Movement Coordination, Figure 1

Dynamics of the HKB model at the coordinative, relative phase (ϕ) level as a function of the control parameter $k = \frac{b}{a}$. *Top row:* Phase space plots $\dot{\phi}$ as a function of ϕ . *Middle:* Landscapes of the potential function $V(\phi)$. *Bottom:* Bifurcation diagram, where *solid lines with filled circles* correspond to stable fixed points (attractors) and *dashed lines with open circles* denote repellers. Note that k increases from right ($k = 0$) to left ($k = 0.75$)

271 portraits as they are just a different representation of the
 272 dynamics. However, the strong hysteresis is more intuitive
 273 in the potential landscape than in phase space, and can
 274 best be seen through an experiment that starts out with
 275 slow movements in anti-phase (indicated by the gray ball
 276 in the minimum of the potential at $\phi = \pi$) and increasing
 277 rate. After passing the critical value $k_c = 0.25$ the slight-
 278 est perturbation will put the ball on the downhill slope
 279 and initiate a switch to in-phase. If the movement is now
 280 slowed down again, going from right to left in the plots,
 281 even though the minimum at $\phi = \pi$ reappears, the ball
 282 cannot jump up and occupy it but will stay in the deep
 283 minimum at $\phi = 0$.

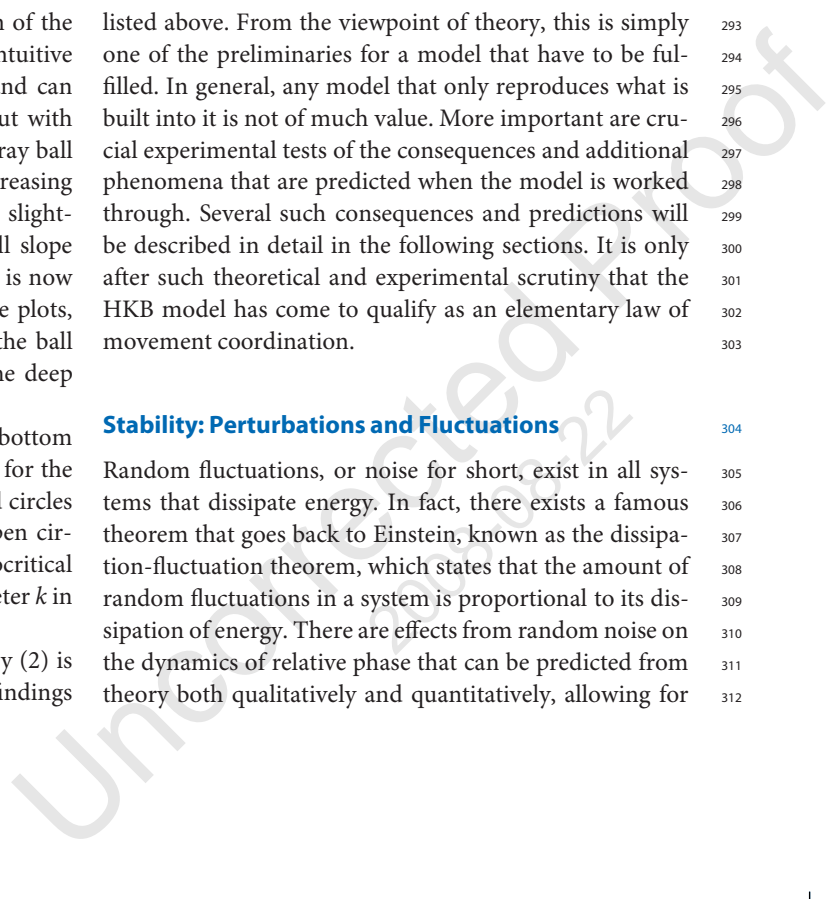
284 Finally, a bifurcation diagram is shown at the bottom
 285 of Fig. 1, where the locations of stable fixed points for the
 286 relative phase ϕ are plotted as solid lines with solid circles
 287 and unstable fixed points as dashed lines with open circles.
 288 Around $k_c = 0.25$ the system undergoes a subcritical
 289 pitchfork bifurcation. Note that the control parameter k in
 290 this plot increases from right to left.

291 Evidently, the dynamical system represented by (2) is
 292 capable of reproducing the basic experimental findings

293 listed above. From the viewpoint of theory, this is simply
 294 one of the preliminaries for a model that have to be ful-
 295 filled. In general, any model that only reproduces what is
 296 built into it is not of much value. More important are crucial
 297 experimental tests of the consequences and additional
 298 phenomena that are predicted when the model is worked
 299 through. Several such consequences and predictions will
 300 be described in detail in the following sections. It is only
 301 after such theoretical and experimental scrutiny that the
 302 HKB model has come to qualify as an elementary law of
 303 movement coordination.

Stability: Perturbations and Fluctuations

304 Random fluctuations, or noise for short, exist in all sys-
 305 tems that dissipate energy. In fact, there exists a famous
 306 theorem that goes back to Einstein, known as the dissipa-
 307 tion-fluctuation theorem, which states that the amount of
 308 random fluctuations in a system is proportional to its dis-
 309 sipation of energy. There are effects from random noise on
 310 the dynamics of relative phase that can be predicted from
 311 theory both qualitatively and quantitatively, allowing for
 312



the HKB model's coordination level to be tested experimentally. Later the individual component level will be discussed.

An essential difference between the dynamical systems approach to movement coordination and the motor program or internal model hypotheses is most distinct in regions where the coordination pattern undergoes a spontaneous qualitative change as in the switch from anti-phase to in-phase in Kelso's experiment. From the latter point of view, these switches simply happen, very much like in the automatic transmission of a car: whenever certain criteria are fulfilled, the transmission switches from one gear to another. It is easy to imagine a similar mechanism to be at work and in control of the transitions in movements: as soon as a certain rate is exceeded, the anti-phase program is somehow replaced by the in-phase module, which is about all we can say regarding the mechanism of switching. On the other hand, by taking dynamic systems theory seriously, one can predict and test phenomena accompanying second-order phase transitions. Three of these phenomena, namely, critical slowing down, enhancement of fluctuations and critical fluctuations will be discussed here in detail.

For a quantitative treatment it is advantageous to expand $\dot{\phi}$ and $V(\phi)$ in (6) into Taylor series around the fixed point $\phi = \pi$ and truncate them after the linear and quadratic terms, respectively

$$\begin{aligned}\dot{\phi} &= -\sin \phi - 2k \sin 2\phi \\ &= -\{-(\phi - \pi) + \dots\} - 2k\{2(\phi - \pi) + \dots\} \\ &\approx (1 - 4k)(\phi - \pi) \\ V(\phi) &= -\cos \phi - k \cos 2\phi \\ &= -\{-1 + (\phi - \pi)^2 + \dots\} \\ &\quad - k\{1 - 4(\phi - \pi)^2 + \dots\} \\ &\approx 1 - k - (1 - 4k)(\phi - \pi)^2.\end{aligned}\tag{7}$$

A typical situation that occurs when a system approaches and passes through a transition point is shown in Fig. 2. In the top row the potential function for $\phi \geq 0$ is plotted (dashed line) together with its expansion around the fixed point $\phi = \pi$ (solid). The bottom row consists of plots of time series showing how the fixed point is or is not approached when the system is initially at $\phi = \pi + \Delta$. The phenomena accompanying second-order phase transitions in a system that contains random fluctuations can be best described by Fig. 2.

Critical slowing down corresponds to the time it takes the system to recover from a small perturbation Δ . In the vicinity of the fixed point the dynamics can be described by the linearization of the nonlinear equation

around the fixed point (7). Such a linear equation can be readily solved leading to

$$\phi(t) = \pi + \Delta e^{(1-4k)t}.$$

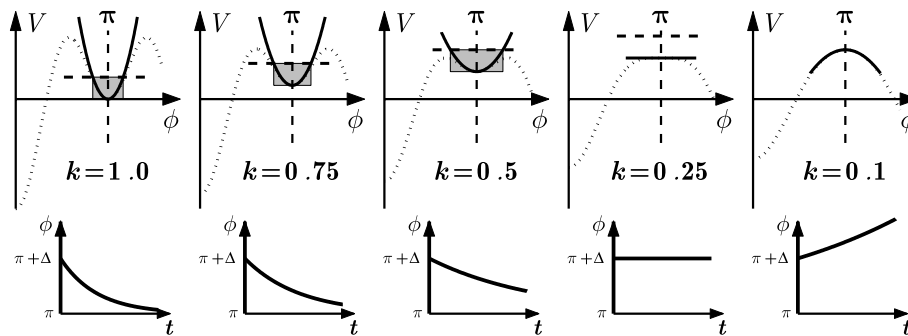
As long as k is larger than its critical value $k_c = 0.25$ the exponent is negative and a perturbation will decay exponentially in time. However, as the system approaches the transition point, this decay will take longer and longer as shown in the bottom row in Fig. 2. At the critical parameter $k = 0.25$ the system will no longer return to the former stable fixed point and beyond that value it will even move away from it. In the latter parameter region the linear approximation is no longer valid. Critical slowing down can be and has been tested experimentally by perturbing a coordination state and measuring the relaxation constant as a function of movement rate prior to the transition. The experimental findings [31,44,45] are in remarkable agreement with the theoretical predictions of coordination dynamics.

Enhancement of fluctuations is to some extent the stochastic analog to critical slowing down. The random fluctuations that exist in all dissipative systems are a stochastic force that kicks the system away from the minimum and (on average) up to a certain elevation in the potential landscape, indicated by the shaded areas in Fig. 2. For large values of k the horizontal extent of this area is small but becomes larger and larger when the transition point is approached. Assuming that the strength of the random force does not change with the control parameter, the standard deviation of the relative phase is a direct measure of this enhancement of fluctuations and will be increasing when the control parameter is moving towards its critical value. Again experimental tests are in detailed agreement with the stochastic version of the HKB model [30,44].

Critical fluctuations can induce transitions even when the critical value of the control parameter has not been reached. As before, random forces will kick the system around the potential minimum and up to (on average) a certain elevation. If this height is larger than the hump it has to cross, as is the case illustrated in Fig. 2 for $k = 0.5$, a transition will occur, even though the fixed point is still classified as stable. In excellent agreement with theory, such critical fluctuations were observed in the original experiments by Kelso and colleagues and have been found in a number of related experimental systems [31,42].

All these hallmarks point to the conclusion that transitions in movement coordination are not simply a switch-

CE2 Is my change here ok?



Movement Coordination, Figure 2

Hallmarks of a system that approaches a transition point: enhancement of fluctuations, indicated by the increasing size of the shaded area; critical slowing down shown by the time it takes for the system to recover from a perturbation (bottom); critical fluctuations occur where the top of the shaded area is higher than the closest maximum in the potential, initiating a switch even though the system is still stable

ing of gears but take place in a well defined way via the instability of a former stable coordination state. Such phenomena are also observed in systems in physics and other disciplines where in situations far from thermal equilibrium macroscopic patterns emerge or change, a process termed self-organization. A general theory of self-organizing systems, called synergetics [17,18], was formulated by Hermann Haken in the early 1970s.

The Oscillator Level

The foregoing description and analysis of bimanual movement coordination takes place on the coordinative or collective level of relative phase. Looking at an actual experiment, there are two fingers moving back and forth and one may ask whether it is possible to find a model on the level of the oscillatory components from which the dynamics of the relative phase can then be derived. The challenge for such an endeavor is at least twofold: first, one needs a dynamical system that accurately describes the movements of the individual oscillatory components (the fingers). Second, one must find a coupling function for these components that leads to the correct relation for the relative phase (2).

Oscillators for Limb Movements

In terms of oscillators there is quite a variety to choose from as most second order systems of the form

$$\ddot{x} + \gamma \dot{x} + \omega^2 x + N(x, \dot{x}) = 0 \tag{8}$$

are potential candidates. Here ω is the angular frequency, γ the linear damping constant and $N(x, \dot{x})$ is a function containing nonlinear terms in x and \dot{x} .

Best known and most widely used are the harmonic oscillators, where $N(x, \dot{x}) = 0$, in particular for the case without damping $\gamma = 0$. In the search for a model to describe human limb movements, however, harmonic oscillators are not well suited, because they do not have stable limit cycles. The phase space portrait of an harmonic oscillator is a circle (or ellipse), but only if it is not perturbed. If such a system is slightly kicked off the trajectory it is moving on, it will not return to its original circle but continue to move on a different orbit. In contrast, it is well known that if a rhythmic human limb movement is perturbed, this perturbation decreases exponentially in time and the movement returns to its original trajectory, a stable limit cycle, which is an object that exists only for nonlinear oscillators [26,45].

Obviously, the amount of possible nonlinear terms to choose from is infinite and at first sight, the task to find the appropriate ones is like looking for a needle in a haystack. However, there are powerful arguments that can be made from both theoretical reasoning and experimental findings, that restrict the nonlinearities, as we shall see, to only two. First, we assume that the function $N(x, \dot{x})$ takes the form of a polynomial in x and \dot{x} and that this polynomial is of the lowest possible order. So the first choice would be to assume that N is quadratic in x and \dot{x} leading to an oscillator of the form

$$\ddot{x} + \gamma \dot{x} + \omega^2 x + ax^2 + b\dot{x}^2 + cx\dot{x} = 0. \tag{9}$$

How do we decide whether (9) is a good model for rhythmic finger movements? If a finger is moved back and forth, that is, performs an alternation between flexion and extension, then this process is to a good approximation symmetric: flexion is the mirror image of extension. In the equations a mirror operation is carried out by substituting x

466 by $-x$, and, in doing so, the equation of motion must not
467 change for symmetry to be preserved. Applied to (9) this
468 leads to

$$469 \begin{aligned} & -\ddot{x} + \gamma(-\dot{x}) + \omega^2(-x) + a(-x)^2 + b(-\dot{x})^2 \\ & + c(-x)(-\dot{x}) = 0 \\ 470 & -\ddot{x} - \gamma\dot{x} - \omega^2x + ax^2 + b\dot{x}^2 + cx\dot{x} = 0 \quad (10) \\ 471 & \ddot{x} + \gamma\dot{x} + \omega^2x - ax^2 - b\dot{x}^2 - cx\dot{x} = 0 \end{aligned}$$

470 where the last equation in (10) is obtained by multiplying
471 the second equation by -1 . It is evident that this equa-
472 tion is not the same as (9). In fact, it is only the same if
473 $a = b = c = 0$, which means that there must not be any
474 quadratic terms in the oscillator equation if one wants
475 to preserve the symmetry between flexion and extension
476 phases of movement. The argument goes even further:
477 $N(x, \dot{x})$ must not contain any terms of even order in x and
478 \dot{x} as all of them, like the quadratic ones, would break the
479 required symmetry. It is easy to convince oneself that as
480 far as the flexion-extension symmetry is concerned all odd
481 terms in x and \dot{x} are fine.

482 There are four possible cubic terms, namely \dot{x}^3 , $\dot{x}x^2$,
483 $x\dot{x}^2$ and x^3 leading to a general oscillator equation of the
484 form

$$485 \ddot{x} + \gamma\dot{x} + \omega^2x + \delta\dot{x}^3 + \epsilon\dot{x}x^2 + ax^3 + bx\dot{x}^2 = 0. \quad (11)$$

486 The effects that these nonlinear terms exert on the oscilla-
487 tor dynamics can be best seen by rewriting (11) as

$$488 \ddot{x} + \dot{x} \underbrace{\{\gamma + \epsilon x^2 + \delta \dot{x}^2\}}_{\text{damping}} + x \underbrace{\{\omega^2 + ax^2 + b\dot{x}^2\}}_{\text{frequency}} = 0 \quad (12)$$

489 which shows that the terms \dot{x}^3 and $\dot{x}x^2$ are position and
490 velocity dependent changes to the damping constant γ ,
491 whereas the nonlinearities x^3 and $x\dot{x}^2$ mainly influence the
492 frequency. As the nonlinear terms were introduced to ob-
493 tain stable limit cycles and the main interest is in ampli-
494 tude and not frequency, we will let $a = b = 0$, which re-
495 duces the candidate oscillators to

$$496 \ddot{x} + \dot{x}\{\gamma + \epsilon x^2 + \delta \dot{x}^2\} + \omega^2x = 0. \quad (13)$$

497 Nonlinear oscillators with either $\delta = 0$ or $\epsilon = 0$ have been
498 studied for a long time and have been termed in the litera-
499 ture as van-der-Pol and Rayleigh oscillator, respectively.

500 Systems of the form (13) only show sustained oscilla-
501 tions on a stable limit cycle within certain ranges of the
502 parameters, as can be seen easily for the van-der-Pol oscil-
503 lator, given by (13) with $\delta = 0$

$$504 \ddot{x} + \dot{x} \underbrace{\{\gamma + \epsilon x^2\}}_{\tilde{\gamma}} + \omega^2x = 0. \quad (14)$$

The underbraced term in (14) represents the effective
505 damping constant, $\tilde{\gamma}$, now depending on the square of the
506 displacement, x^2 , a quantity which is non-negative. For the
507 parameters γ and ϵ one can distinguish the following four
508 cases:
509

510 $\gamma > 0, \epsilon > 0$ The effective damping $\tilde{\gamma}$ is always positive.
511 The trajectories are evolving towards the origin, which
512 is a stable fixed point.

513 $\gamma < 0, \epsilon < 0$ The effective damping $\tilde{\gamma}$ is always negative.
514 The system is unstable and the trajectories are evolving
515 towards infinity.

516 $\gamma > 0, \epsilon < 0$ For small values of the amplitude x^2 the ef-
517 fective damping $\tilde{\gamma}$ is positive leading to even smaller
518 amplitudes. For large values of x^2 the effective damp-
519 ing $\tilde{\gamma}$ is negative leading to a further increase in ampli-
520 tude. The system evolves either towards the fixed point
521 or towards infinity depending on the initial conditions.

522 $\gamma < 0, \epsilon > 0$ For small values of the amplitude x^2 the ef-
523 fective damping $\tilde{\gamma}$ is negative leading to an increase in
524 amplitude. For large values of x^2 the effective damping
525 $\tilde{\gamma}$ is positive and decreases the amplitude. The system
526 evolves towards a stable limit cycle.

The main features for the van-der-Pol oscillator are
527 shown in Fig. 3 with the time series (left), the phase space
528 portrait (middle) and the power spectrum (right). The
529 time series is not a sine function but has a fast rising in-
530 creasing flank and a more shallow slope on the decreasing
531 side. Such time series are called relaxation oscillations. The
532 trajectory in phase space is closer to a rectangle than to
533 a circle and the power spectrum shows pronounced peaks
534 at the fundamental frequency ω and its odd higher har-
535 monics ($3\omega, 5\omega, \dots$).
536

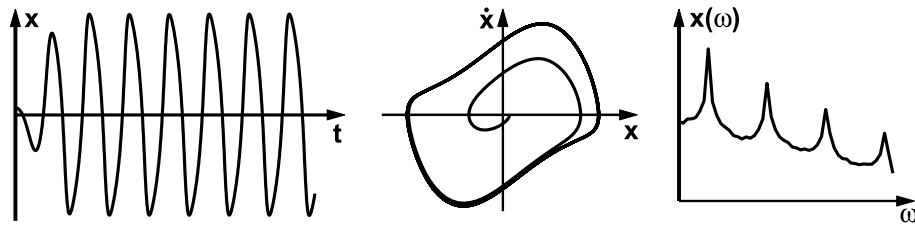
537 In contrast to the van-der-Pol case the damping con-
538 stant $\tilde{\gamma}$ for the Rayleigh oscillator, the case $\epsilon = 0$ in (13),
539 depends on the square of the velocity \dot{x}^2 . Arguments
540 similar to those above lead to the conclusion that the
541 Rayleigh oscillator shows sustained oscillations for param-
542 eters $\gamma < 0$ and $\delta > 0$.

543 As shown in Fig. 4 the time series and trajectories of
544 the Rayleigh oscillator also exhibit relaxation behavior, but
545 in this case with a slow rise and fast drop. As for the
546 van-der-Pol, the phase space portrait is almost rectangu-
547 lar but the long and short axes are switched. Again the
548 power spectrum has peaks at the fundamental frequency
549 and contains odd higher harmonics.

550 Evidently, taken by themselves neither the van-der-Pol
551 nor Rayleigh oscillators are good models for human limb
552 movement for at least two reasons, even though they ful-
553 fill one requirement for a model: they have stable limit cy-
554 cles. First, human limb movements are almost sinusoidal



Unauthenticated Proof



Movement Coordination, Figure 3

The van-der-Pol oscillator: time series (left), phase space trajectory (middle) and power spectrum (right)

555 and their trajectories have a circular or elliptical shape.
 556 Second, it has also been found in experiments with hu-
 557 man subjects performing rhythmic limb movements that
 558 when the movement rate is increased the amplitude of the
 559 movement decreases linearly with frequency [25]. It can be
 560 shown that for the van-der-Pol oscillator the amplitude is
 561 independent of frequency and for the Rayleigh it decreases
 562 proportional to ω^{-2} , both in disagreement with the exper-
 563 imental findings.

564 It turns out that a combination of the van-der-Pol
 565 and Rayleigh oscillator, termed the hybrid oscillator of the
 566 form (13) fulfills all the above requirements if the param-
 567 eters are chosen as $\gamma < 0$ and $\epsilon \approx \delta > 0$.

568 As shown in Fig. 5 the time series for the hybrid oscilla-
 569 tor is almost sinusoidal and the trajectory is elliptical. The
 570 power spectrum has a single peak at the fundamental fre-
 571 quency. Moreover, the relation between the amplitude and
 572 frequency is a linear decrease in amplitude when the rate is
 573 increased as shown schematically in Fig. 6. Taken together,
 574 the hybrid oscillator is a good approximation for the tra-
 575 jectories observed experimentally in human limb move-
 576 ments.

577 The Coupling

578 As pointed out already, in a second step one has to find
 579 a coupling function between two hybrid oscillators that
 580 leads to the correct dynamics for the relative phase (2).
 581 The most common realization of a coupling between
 582 two oscillators is a spring between two pendulums, lead-
 583 ing to a force proportional to the difference in locations
 584 $f_{12} = k[x_1(t) - x_2(t)]$. It can easily be shown, that such
 585 a coupling does not lead to the required dynamics on the
 586 relative phase level. In fact, several coupling terms
 587 have been suggested that do the trick, but none of them
 588 is very intuitive. The arguably easiest form, which is one
 589 of the possible couplings presented in the original HKB
 590 model [19], is given by

$$591 \quad f_{12} = (\dot{x}_1 - \dot{x}_2)\{\alpha + \beta(x_1 - x_2)^2\}. \quad (15)$$

592 Combined with two of the hybrid oscillators, the dynamical
 593 system that describes the transition from anti-phase to
 594 in-phase in bimanual finger movements takes the form

$$\begin{aligned} \ddot{x}_1 + \dot{x}_1(\gamma + \epsilon x_1^2 + \delta \dot{x}_1^2) + \omega^2 x_1 &= (\dot{x}_1 - \dot{x}_2)\{\alpha + \beta(x_1 - x_2)^2\} \\ \ddot{x}_2 + \dot{x}_2(\gamma + \epsilon x_2^2 + \delta \dot{x}_2^2) + \omega^2 x_2 &= (\dot{x}_2 - \dot{x}_1)\{\alpha + \beta(x_2 - x_1)^2\}. \end{aligned} \quad (16)$$

595 A numerical simulation of (16) is shown in Fig. 7. In
 596 the top row the amplitudes x_1 and x_2 are plotted as a func-
 597 tion of time. The movement starts out in anti-phase at
 598 $\omega = 1.4$ and the frequency is continuously increased to
 599 a final value of $\omega = 1.8$. At a critical rate ω_c the anti-
 600 phase pattern becomes unstable and a transition to in-
 601 phase takes place. At the bottom a **point** estimate of the
 602 relative phase $\phi(t)$ is shown calculated as

$$603 \quad \phi(t) = \varphi_1(t) - \varphi_2(t) = \arctan \frac{\dot{x}_1}{x_1} - \arctan \frac{\dot{x}_2}{x_2}. \quad (17)$$

604 The relative phase changes from a value of π during the
 605 anti-phase movement to $\phi = 0$ when the in-phase pattern
 606 has been established.

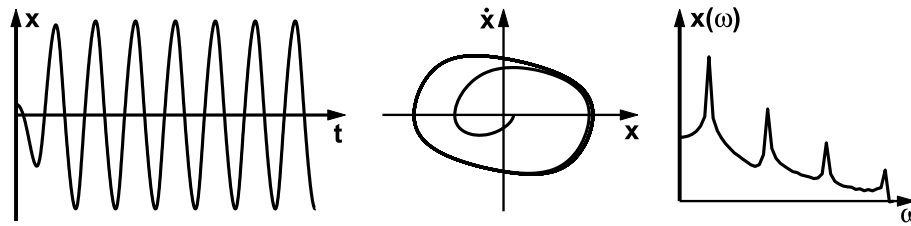
607 To derive the phase relation (2) from (16) is a little
 608 lengthy but straightforward by using the ansatz (hypothesis)
 609

$$610 \quad x_k(t) = A_k(t)e^{i\omega t} + A_k^*(t)e^{-i\omega t} \quad (18)$$

611 then calculating the derivatives and inserting them
 612 into (16). ~~Then the~~ slowly varying amplitude approxima-
 613 tion ($\dot{A}(t) \ll \omega$) and rotating wave approximation (neg-
 614 lect all frequencies $> \omega$) are applied. Finally, introducing
 615 the relative phase $\phi = \varphi_1 - \varphi_2$ after writing $A_k(t)$ in the
 616 form

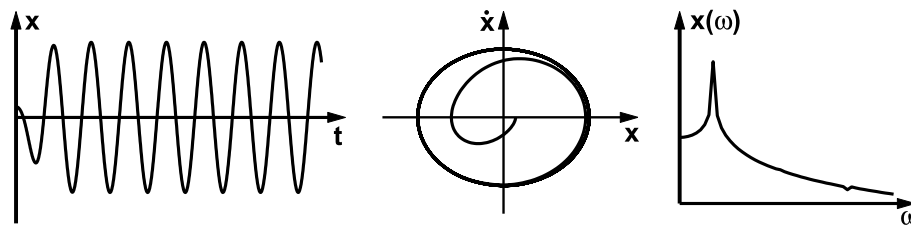
$$617 \quad A_k(t) = r e^{i\varphi_k(t)} \quad (19)$$

618 leads to a relation for the relative phase ϕ of the form (2)
 619 from which the parameters a and b can be readily found
 620



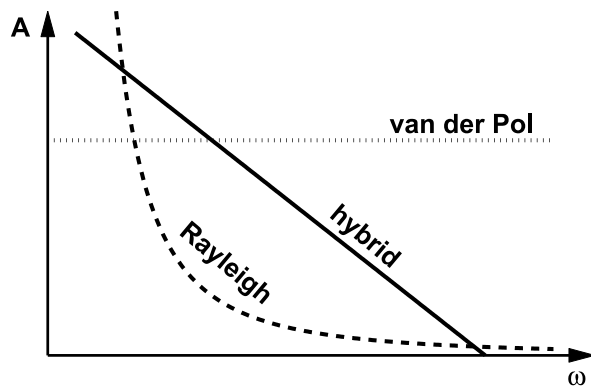
Movement Coordination, Figure 4

The Rayleigh oscillator: time series (left), phase space trajectory (middle) and power spectrum (right)



Movement Coordination, Figure 5

The hybrid oscillator: time series (left), phase space trajectory (middle) and power spectrum (right)



Movement Coordination, Figure 6

Amplitude-frequency relation for the van-der-Pol (dotted), Rayleigh ($\sim \omega^{-2}$, dashed) and hybrid ($\sim -\omega$, solid) oscillator

dinating components are identical, like two index fingers. As a consequence, the coupled system (16) has a symmetry: it stays invariant if we replace x_1 by x_2 and x_2 by x_1 . For the coordination between two limbs that are not the same like an arm and a leg, this symmetry no longer exists – it is said to be broken. In terms of the model, the main difference between an arm and a leg is that they have different eigenfrequencies, so the oscillator frequencies ω in (16) are no longer the same but become ω_1 and ω_2 . This does not necessarily mean that during the coordination the components oscillate at different frequencies; they are still coupled, and this coupling leads to a common frequency Ω , at least as long as the eigenfrequency difference is not too big. But still, a whole variety of new phenomena originates from such a breaking of the symmetry between the components [5,22,23,29,37].

As mentioned in Subsect. “The Coupling” the dynamics for the relative phase can be derived from the level of coupled oscillators (16) for the case of the same eigenfrequencies. Performing the same calculations for two oscillators with frequencies ω_1 and ω_2 leads to an additional term in (2), which turns out to be a constant, commonly called $\delta\omega$. With this extension the equation for the relative phase reads

in terms of the parameters that describe the oscillators and their coupling in (16)

$$a = -\alpha - 2\beta r^2, \quad b = \frac{1}{2}\beta r^2$$

$$\text{with } r^2 = \frac{-\gamma + \alpha(1 - \cos \phi)}{\epsilon + 3\delta\omega^2 - 2\beta(1 - \cos \phi)^2}. \quad (20)$$

627 Breaking and Restoring Symmetries

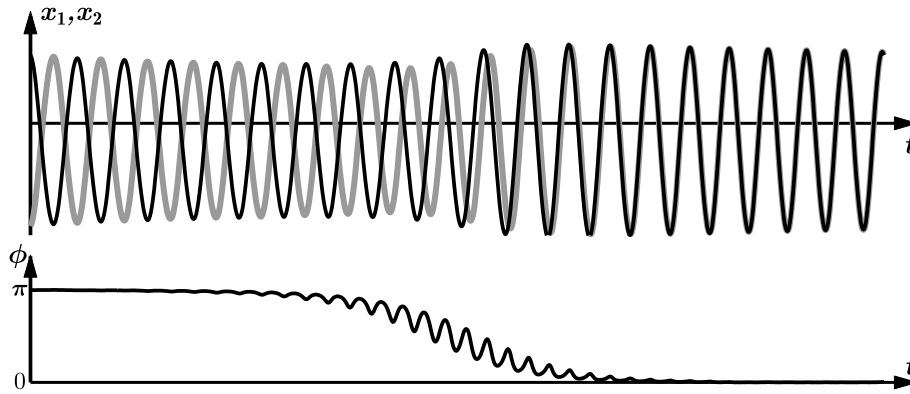
628 Symmetry Breaking Through the Components

629 For simplicity, the original HKB model assumes on both
630 the oscillator and the relative phase level that the two coor-

$$\dot{\phi} = \delta\omega - a \sin \phi - 2b \sin 2\phi$$

$$\text{with } \delta\omega = \frac{\omega_1^2 - \omega_2^2}{\Omega} \approx \omega_1 - \omega_2. \quad (21)$$

Uncorrected Proof



Movement Coordination, Figure 7

Simulation of (16) where the frequency ω is continuously increased from $\omega = 1.4$ on the left to $\omega = 1.8$ on the right. *Top*: time series of the amplitudes x_1 and x_2 undergoing a transition from anti-phase to in-phase when ω exceeds a critical value. *Bottom*: **Point** estimate of the relative phase ϕ changing from an initial value of π during anti-phase to 0 when the in-phase movement is established. Parameters: $\gamma = -0.7$, $\epsilon = \delta = 1$, $\alpha = -0.2$, $\beta = 0.2$, and $\omega = 1.4$ to 1.8

659 The exact form for the term $\delta\omega$ turns out to be the dif-
 660 ference of the squares of the eigenfrequencies divided by
 661 the rate Ω the oscillating frequency of the coupled system,
 662 which simplifies to $\omega_1 - \omega_2$ if the frequency difference is
 663 small. As before (21) can be scaled, which eliminates one
 664 of the parameters, and $\dot{\phi}$ can be derived from a potential
 665 function

$$\begin{aligned} \dot{\phi} &= \delta\omega - \sin \phi - 2k \sin 2\phi \\ &\equiv \frac{dV(\phi)}{d\phi} \text{ with } V(\phi) = -\delta\omega \phi - \cos \phi - k \cos 2\phi . \end{aligned} \quad (22)$$

667 Plots of the phase space and the potential landscape for
 668 different values of k and $\delta\omega$ are shown in Figs. 8 and 9, re-
 669 spectively. From these figures it is obvious that the symme-
 670 try breaking leads to a vertical shift of the curves in phase
 671 space and a tilt in the potential functions, which has sev-
 672 eral important consequences for the dynamics. First, for
 673 a nonvanishing $\delta\omega$ the stable fixed points for the relative
 674 phase are no longer located at $\phi = 0$ and $\phi = \pm\pi$ but are
 675 now shifted (see Fig. 8). The amount of this shift can be
 676 calculated for small values of $\delta\omega$ and new locations for the
 677 stable fixed points are given by

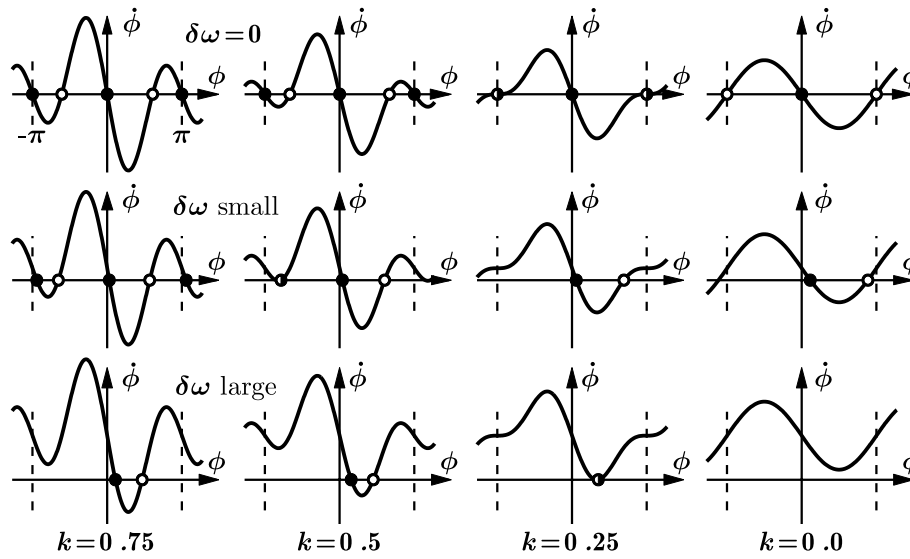
$$\phi^{(0)} = \frac{\delta\omega}{1 + 4k} \quad \text{and} \quad \phi^{(\pi)} = \pi - \frac{\delta\omega}{1 - 4k} . \quad (23)$$

679 Second, for large enough values of $\delta\omega$ not only the fixed
 680 point close to $\phi = \pi$ becomes unstable but also the in-
 681 phase pattern loses stability undergoing a saddle node bi-
 682 furcation as can be seen in the bottom row in Fig. 8. Be-
 683 yond this point there are no stable fixed points left and

the relative phase will not settle down at a fixed value any-
 more but exhibit phase wrapping. However, this wrapping
 does not occur with a constant angular velocity, which can
 best be seen in the plot on the bottom right in Fig. 9. As
 the change in relative phase $\dot{\phi}$ is the negative derivative of
 the potential function, it is given by the slope. This slope
 is large and almost constant for negative values of ϕ , but
 for small positive values, where the in-phase fixed point
 was formerly located, the slope becomes less steep indicat-
 ing that ϕ changes more slowly in this region before the
 dynamics picks up speed again when approaching π . So
 even as the fixed point has disappeared the dynamics still
 shows reminiscence of its former existence.

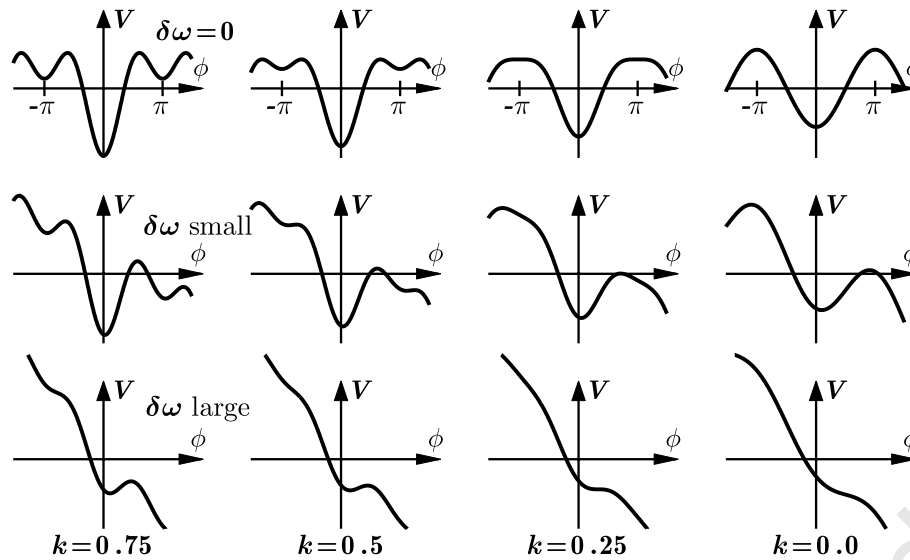
The dynamics of relative phase for the case of differ-
 ent eigenfrequencies from a simulation of (22) is shown
 in Fig. 10. Starting out at a slow movement rate on the
 left, the system settles into the fixed point close to $\phi = \pi$.
 When the movement rate is continuously increased, the
 fixed point drifts upwards. At a first critical point a transi-
 tion to in-phase takes place, followed by another drift, this
 time for the fixed point representing the in-phase move-
 ment. Finally, this state also loses stability and the relative
 phase goes into wrapping. Reminiscence in the phase re-
 gions of the former fixed point are still visible by a flatten-
 ing of the slope around $\phi \approx \pi$. With a further increase of
 the movement rate the function approaches a straight line.

The third consequence of this symmetry breaking is
 best described using the potential function for small values
 of $\delta\omega$ compared to the symmetric case $\delta\omega = 0$. For the lat-
 ter, when the system is initially in anti-phase $\phi = \pi$ and k
 is decreased through its critical value a switch to in-phase
 takes place as was shown in Fig. 1 (middle row). However,



Movement Coordination, Figure 8

Phase space plots for different values of the control parameters k and $\delta\omega$. With increasing asymmetry (top to bottom) the functions are shifted more and more upwards leading to an elimination of the fixed points near $\phi = -\pi$ and $\phi = 0$ via saddle node bifurcations at $k = 0.5$ for small $\delta\omega$ and $k = 0.25$ for $\delta\omega$ large, respectively

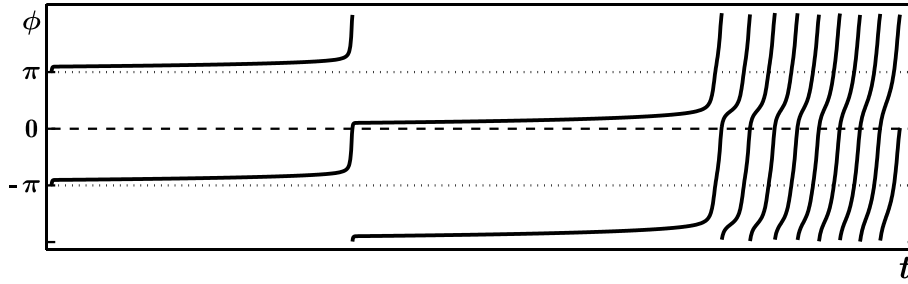


Movement Coordination, Figure 9

Potential landscape for different values of the control parameters k and $\delta\omega$. With increasing asymmetry (top to bottom) the functions get more and more tilted, destabilizing the system up to a point where there are no fixed points left on the bottom right. However, remnants of the fixed point can still be seen as changes in the curvature of the potential

716 the ball there does not necessarily have to roll to the left
 717 towards $\phi = 0$ but with the same probability could roll to
 718 the right ending up in the minimum that exists at $\phi = 2\pi$
 719 and also represents an in-phase movement. Whereas the
 720 eventual outcome is the same because due to the periodic-

ity $\phi = 0$ and $\phi = 2\pi$ are identical, the two paths can very
 721 well be distinguished. The curve in Fig. 7 (bottom), showing
 722 the point estimate of the relative phase during a transition,
 723 goes from $\phi = \pi$ down to $\phi = 0$, but could, in fact
 724 with the same probability, go up towards $\phi = 2\pi$. In con-
 725



Movement Coordination, Figure 10

Relative phase ϕ as a function of time. Shown is a 4π plot of a simulation of (22) for $\delta\omega = 1.7$ where the control parameter k is continuously decreased from $k = 2$ on the left to $k = 0$ on the right. The system settles close to anti-phase and the fixed point drifts as k is decreased (corresponding to a faster period of oscillation). At a first critical value a transition to in-phase takes place followed by another fixed point drift. Finally, the in-phase fixed point disappears and the phase starts wrapping

726 trast, if the eigenfrequencies are different, also the points
 727 $-\pi$ and π , and 0 and 2π are no longer the same. If the
 728 system is in anti-phase at $\phi = \pi$ and k is decreased, it is
 729 evident from the middle row in Fig. 9 that a switch will
 730 not take place towards the left to $\phi \approx 0$, as the dynam-
 731 ics would have to climb over a potential hill to do so. As
 732 there are random forces acting on the dynamics a switch
 733 to $\phi \approx 0$ will still happen from time to time, but it is not
 734 equally probable to a transition to $\phi \approx 2\pi$, and it becomes
 735 even more unlikely with increasing $\delta\omega$.

736 These consequences, theoretically predicted to occur
 737 when the symmetry between the oscillating components is
 738 broken, can and have been tested, and have been found to
 739 be in agreement with the experimental results [21,29].

Asymmetry in the Mode of Coordination

741 Even though (16) is symmetric in the coordinating com-
 742 ponents it can only describe a transition from anti-phase
 743 to in-phase but not the other way around. Equation (16)
 744 is highly asymmetric with respect to coordination mode.
 745 This can be seen explicitly when we introduce variables
 746 that directly reflect modes of coordination

$$747 \quad \psi_+ = x_1 + x_2 \quad \text{and} \quad \psi_- = x_1 - x_2. \quad (24)$$

748 For an in-phase movement we have $x_1 = x_2$ and ψ_-
 749 vanishes, whereas for anti-phase $x_1 = -x_2$ and therefore
 750 $\psi_+ = 0$. We can now derive the dynamics in the variables
 751 ψ_+ and ψ_- by expressing the original displacements as

$$752 \quad x_1 = \frac{1}{2}(\psi_+ + \psi_-) \quad \text{and} \quad x_2 = \frac{1}{2}(\psi_+ - \psi_-) \quad (25)$$

and inserting them into (16), which leads to

$$\begin{aligned} \ddot{\psi}_+ + \epsilon\dot{\psi}_+ + \omega^2\psi_+ + \frac{\gamma}{12} \frac{d}{dt} (\psi_+^3 + 3\psi_+\psi_-^2) \\ + \frac{\delta}{4} (\dot{\psi}_+^3 + 3\dot{\psi}_+\dot{\psi}_-^2) = 0 \\ \ddot{\psi}_- + \epsilon\dot{\psi}_- + \omega^2\psi_- + \frac{\gamma}{12} \frac{d}{dt} (\psi_-^3 + 3\psi_-\psi_+^2) \\ + \frac{\delta}{4} (\dot{\psi}_-^3 + 3\dot{\psi}_-\dot{\psi}_+^2) \\ = 2\dot{\psi}_-(\alpha + \beta\psi_-^2). \end{aligned} \quad (26)$$

753 The asymmetry between in-phase and anti-phase is evi-
 754 dent from (26), as the right-hand side of the first equation
 755 vanishes and the equation is even independent of the cou-
 756 pling parameters α and β . This is the reason that the origi-
 757 nal HKB model only shows transitions from anti-phase to
 758 in-phase and not vice versa.
 759
 760

Transitions to Anti-phase

761 In 2000 Carson and colleagues [6] published results from
 762 an experiment in which subjects performed bimanual
 763 pronation-supination movements paced by a metronome
 764 of increasing rate (see also [2]). In this context an anti-
 765 phase movement corresponds to the case where one arm
 766 performs a pronation while the other arm is supinat-
 767 ing. Correspondingly, pronation and supination with both
 768 arms at the same time represents in-phase. In their exper-
 769 iment Carson et al. used a manipulandum that allowed for
 770 changing the axis of rotation individually for both arms as
 771 shown in Fig. 11a. With increasing movement rate sponta-
 772 neous transitions from anti-phase to in-phase, but not vice
 773 versa, were found when the subjects performed prona-
 774 tion-supination movements around the same axes for both
 775 arms. In trials where one arm was rotating around the axis
 776

777 above the hand and the other around the one below, anti-
 778 phase was found to be stable and the in-phase movement
 779 underwent a transition to anti-phase as shown for repre-
 780 sentative trials in Fig. 12.

781 It is evident that the HKB model in neither its origi-
 782 nal form (2) nor the mode formulation (26) is a valid
 783 model for these findings. However, Fuchs and Jirsa [11]
 784 showed that by starting from the mode description (26)
 785 it is ~~straight forward~~ to extend HKB such that, depend-
 786 ing on an additional parameter σ , either the in-phase or
 787 the anti-phase mode is a stable movement pattern at high
 788 rates. The additional parameter corresponds to the relative
 789 locations of the axes of rotation in the Carson et al. exper-
 790 iment which can be defined in its easiest form as

$$791 \quad \sigma = \frac{|l_1 - l_2|}{L} \quad (27)$$

792 where l_1, l_2 and L are as shown in Fig. 11b. In fact, any
 793 monotonic function f with $f(0) = 0$ and $f(1) = 1$ is com-
 794 patible with theory and its actual shape has to be deter-
 795 mined experimentally.

796 By looking at the mode Eqs. (26) it is clear ~~that~~ sub-
 797 stitution $\psi_+ \rightarrow \psi_-$ and $\psi_- \rightarrow \psi_+$ to the left-hand side
 798 of the first equation leads to the left-hand side of the sec-
 799 ond equation and vice versa. For the terms on the right-
 800 hand side representing the coupling this is obviously not
 801 the case. Therefore, we now introduce a parameter σ and
 802 additional terms into (26) such that for $\sigma = 0$ these equa-
 803 tions remain unchanged, whereas for $\sigma = 1$ we obtain (26)
 804 with all + and - subscripts reversed

$$805 \quad \begin{aligned} & \ddot{\psi}_+ + \epsilon \dot{\psi}_+ + \omega^2 \psi_+ + \frac{\gamma}{12} \frac{d}{dt} (\psi_+^3 + 3\psi_+ \psi_-^2) \\ & + \frac{\delta}{4} (\dot{\psi}_+^3 + 3\dot{\psi}_+ \dot{\psi}_-^2) = 2\sigma \dot{\psi}_+ (\alpha + \beta \psi_+^2) \\ & \ddot{\psi}_- + \epsilon \dot{\psi}_- + \omega^2 \psi_- + \frac{\gamma}{12} \frac{d}{dt} (\psi_-^3 + 3\psi_- \psi_+^2) \\ & + \frac{\delta}{4} (\dot{\psi}_-^3 + 3\dot{\psi}_- \dot{\psi}_+^2) = 2(1 - \sigma) \dot{\psi}_- (\alpha + \beta \psi_-^2). \end{aligned} \quad (28)$$

806 From (28) it is straight forward to go back to the rep-
 807 resentation of the ~~finger~~ oscillators

$$808 \quad \begin{aligned} \ddot{x}_1 + \dots &= \frac{1}{2} (\ddot{\psi}_+ + \ddot{\psi}_-) + \dots \\ &= \dot{\psi}_- (\alpha + \beta \psi_-^2) + \sigma \{ \dot{\psi}_+ (\alpha + \beta \psi_+^2) \\ & \quad - \dot{\psi}_- (\alpha + \beta \psi_-^2) \} \\ \ddot{x}_2 + \dots &= \frac{1}{2} (\ddot{\psi}_+ - \ddot{\psi}_-) + \dots \\ &= -\dot{\psi}_- (\alpha + \beta \psi_-^2) + \sigma \{ \dot{\psi}_+ (\alpha + \beta \psi_+^2) \\ & \quad + \dot{\psi}_- (\alpha + \beta \psi_-^2) \} \end{aligned} \quad (29)$$

809 where the left-hand side which represents the oscillators
 810 has been written only symbolically as all we are dealing
 811 with is the coupling on the right. Replacing the mode am-
 812 plitudes ψ_+ and ψ_- in (29) using (24) one finds the gen-
 813 eralized coupling as a function of x_1 and x_2

$$814 \quad \begin{aligned} \ddot{x}_1 + \dots &= (\dot{x}_1 - \dot{x}_2) \{ \alpha + \beta (x_1 - x_2)^2 \} \\ & + 2\sigma \{ \alpha \dot{x}_2 + \beta [\dot{x}_2 (x_1^2 + x_2^2) + 2\dot{x}_1 x_1 x_2] \} \\ \ddot{x}_2 + \dots &= (\dot{x}_2 - \dot{x}_1) \{ \alpha + \beta (x_2 - x_1)^2 \} \\ & + 2\sigma \{ \alpha \dot{x}_1 + \beta [\dot{x}_1 (x_1^2 + x_2^2) + 2\dot{x}_2 x_1 x_2] \}. \end{aligned} \quad (30)$$

815 Like the original oscillator Eq. (16), Eq. (30) is invariant
 816 under the exchange of x_1 and x_2 but in addition allows for
 817 transitions from in-phase to anti-phase coordination if the
 818 parameter σ is chosen appropriately ($\sigma = 1$, for instance),
 819 as shown in Fig. 14.

820 As the final step, an equation for the dynamics of rela-
 821 tive phase can be obtained from (30) by performing the
 822 same steps as before, which leads to a modified form of the
 823 HKB equation (2)

$$824 \quad \dot{\phi} = -(1 - 2\sigma)a \sin \phi - 2b \sin 2\phi \quad (31)$$

825 and the corresponding potential function

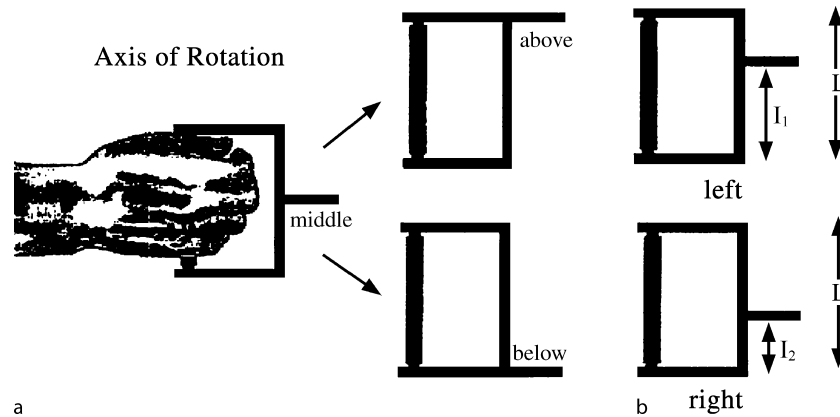
$$826 \quad \begin{aligned} \dot{\phi} &= -\frac{dV(\phi)}{d\phi} \\ \text{with } V(\phi) &= -(1 - 2\sigma)a \cos \phi - b \cos 2\phi. \end{aligned} \quad (32)$$

827 Both equations can be scaled again leading to

$$828 \quad \begin{aligned} \dot{\phi} &= -(1 - 2\sigma) \sin \phi - 2k \sin 2\phi \\ &\equiv \frac{dV(\phi)}{d\phi} \quad \text{with} \end{aligned} \quad (33)$$

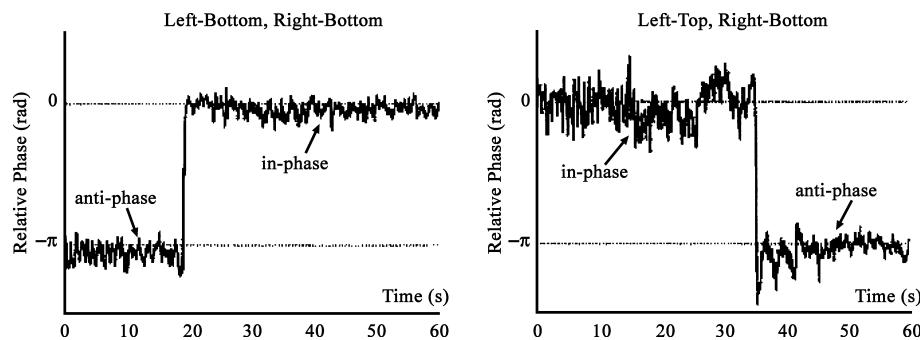
$$829 \quad V(\phi) = -(1 - 2\sigma) \cos \phi - k \cos 2\phi.$$

830 The landscapes of the potential for different values of
 831 the control parameters k and σ are shown in Fig. 15. The
 832 left column exhibits the original HKB case which is ob-
 833 tained for $\sigma = 0$. The functions in the most right column,
 834 representing the situation for $\sigma = 1$, are identical in shape
 835 to the $\sigma = 0$ case, simply shifted horizontally by a value
 836 of π . These two extreme cases are almost trivial and were
 837 the ones originally investigated in the Carson et al. exper-
 838 iment with the axes of rotation either on the same side or
 839 on opposite sides with respect to the hand. As the cor-
 840 responding potential functions are shifted by π with re-
 841 spect to each other, one could assume that for an inter-
 842 mediate value of σ between 0 and 1 the functions are also
 843 shifted, just by a smaller amount. Such horizontal trans-
 844 lations lead to fixed point drifts, as has been seen before
 845



Movement Coordination, Figure 11

Manipulandum used by Carson and colleagues [6]. **a** The original apparatus that allowed for variation in axis of rotation above, below and in the middle of the hand. **b** The axis of rotation can be changed continuously, allowing us to introduce a parameter σ as a quantitative measure for the relative locations of the axes



Movement Coordination, Figure 12

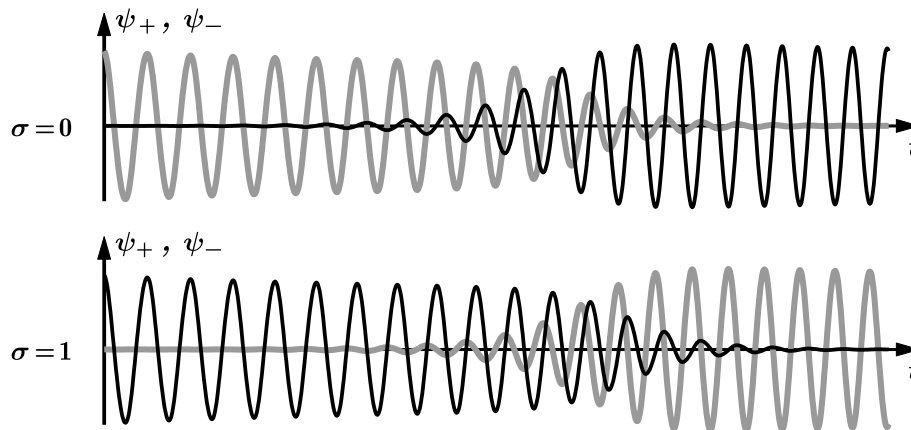
Relative phase over time for two representative trials from the Carson et al. experiment. *Left*: the axis of rotation is below the hand for both arms and a switch from anti-phase to in-phase occurs as the movement speeds up. *Right*: with one axis above and the other below the hand, the in-phase movement becomes unstable at higher rates leading to a transition to anti-phase

847 for oscillation components with different eigenfrequencies. The theory, however, predicts that this is not the case. 848
849 In fact, for $\sigma = 0.5$ theory predicts that the two coordination modes in-phase and anti-phase are equally stable 850
851 for all movement rates. The deep minima for slow rates indicate high stability for both movement patterns and as 852
853 the rate increases both minima become more and more shallow, i. e. both movement patterns become less stable. 854
855 Eventually, for high rates at $k = 0$ the potential is entirely flat, which means that there are no attractive states what- 856
857 soever. Pushed only by the stochastic forces in the system, the relative phase will now undergo a random walk. Note 858
859 that this is very different from the phase wrapping encountered before where the phase was constantly increasing 860
861 due to the lack of an attractive state. Here the relative phase will move back and forth in a purely random fash- 862

863 ion, known in the theory of stochastic systems as Brownian motion. Again experimental evidence exists from the 864
865 Carson group that changing the distance between the axes of rotation gradually leads to the phenomena predicted by 866
867 theory.

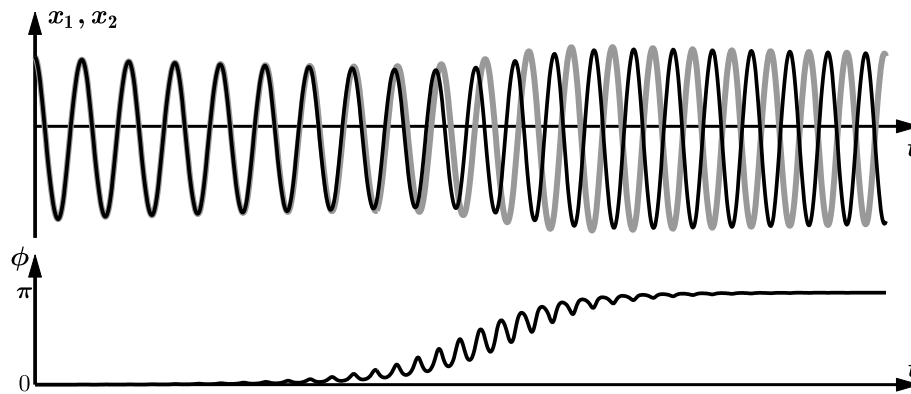
Conclusions

868 The theoretical framework outlined above represents the 869
870 core of the dynamical systems approach to movement coordination. Rather than going through the large variety 871
872 of phenomena that coordination dynamics and the HKB model have been applied to, emphasis has been put on 873
874 a detailed description of the close connection between theoretical models and experimental results. Modeling the 875
876 coordination of movement as dynamical systems on both 876



Movement Coordination, Figure 13

Simulation of (28) for $\sigma = 0$ (top) and $\sigma = 1$ (bottom) where the frequency ω is continuously increased from $\omega = 1.4$ on the left to $\omega = 1.8$ on the right. Time series of the mode amplitudes ψ_+ (black) and ψ_- (gray) undergoing transitions from anti-phase to in-phase (top) and from in-phase to anti-phase (bottom) when ω exceeds a critical value. Parameters: $\gamma = -0.7, \epsilon = \delta = 1, \alpha = -0.2, \beta = 0.2$, and $\omega = 1.4$ to 1.8



Movement Coordination, Figure 14

Simulation of (30) where the frequency ω is continuously increased from $\omega = 1.4$ on the left to $\omega = 1.8$ on the right. Top: time series of the amplitudes x_1 and x_2 undergoing a transition from in-phase to anti-phase when ω exceeds a critical value. Bottom: Point estimate of the relative phase ϕ changing from an initial value of 0 during the in-phase to π when the anti-phase movement is established. Parameters: $\gamma = -0.7, \epsilon = \delta = 1, \alpha = -0.2, \beta = 0.2, \sigma = 1$ and $\omega = 1.4$ to 1.8

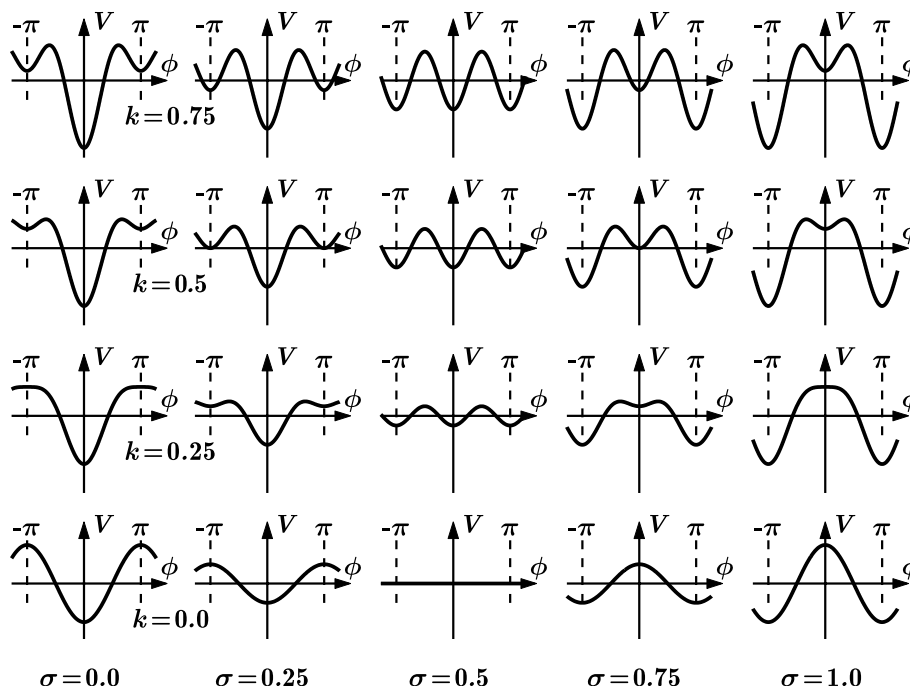
877 the mesoscopic level of the component oscillators and the
 878 macroscopic level of relative phase allowed for quantita-
 879 tive predictions and experimental tests with an accuracy
 880 that is unprecedented in the life sciences, a field where
 881 most models are qualitative and descriptive.

882 **Extensions of the HKB Model**

883 Beyond the phenomena described above, the HKB model
 884 has been extended in various ways. Some of these exten-
 885 sions (by no mean exhaustive) are listed below with a very
 886 brief description; the interested reader is referred to the
 887 literature for details.

- The quantitative description of the influence of noise on the dynamics given in Sect. “Stability: Perturbations and Fluctuations” can be done in a quantitative fashion by adding a stochastic term to (2) [40,43] or its generalizations (21) and (31) [11] and treating them as Langevin equations within the theory of stochastic systems (see e. g. [16] for stochastic systems). In this case the system is no longer described by a single time series for the relative phase but by a probability distribution function. How such distributions evolve in time is then given by the corresponding Fokker-Planck equation and allows for a quantitative description of the

888
 889
 890
 891
 892
 893
 894
 895
 896
 897
 898
 899



Movement Coordination, Figure 15
 Potential landscape for different values of the control parameters k and σ

900 stochastic phenomena such as enhancement of fluctu-
 901 ations and critical fluctuations. An important quantity
 902 that can be derived in this context and is also related to
 903 the critical fluctuations is the mean-first-passage time,
 904 which is the time it takes (on average) to move over
 905 a hump in the potential function.

- 906 • When subjects flex a single finger between the beats
 907 of a metronome, i. e. syncopate with the stimulus, and
 908 the metronome rate is increased, they switch sponta-
 909 neously to a coordination pattern where they flex their
 910 finger on the beat, i. e. synchronize with the stimulus.
 911 This so-called syncopation-synchronization paradigm
 912 introduced by Kelso and colleagues [32] has been fre-
 913 quently used in brain-imaging experiments.
- 914 • A periodic **patterning** CE3 in the time series of the
 915 relative phase was found experimentally in the case of
 916 broken symmetry by Schmidt et al. [41] and suc-
 917 cessfully derived from the oscillator level of the HKB
 918 model [12,14].
- 919 • The metronome pacing can be explicitly included
 920 into (2) and its generalizations [24]. This so-called
 921 parametric driving allows us to explain effects in the
 922 movement trajectory known as anchoring, i. e. the
 923 variability of the movement is smaller around the

924 metronome beat compared to other regions in phase
 925 space [10]. With parametric driving the HKB model
 926 also makes correct predictions for the stability of multi-
 927 frequency coordination, where the metronome cycle
 928 is half of the movement cycle, i. e. there is a beat at
 929 the points of maximum flexion and maximum exten-
 930 sion [1]. There ~~are~~ effects from more complicated
 931 polyrhythms that have been studied [38,39,47].

- 932 • The effect of symmetry breaking has been studied in-
 933 tensively in experiments where subjects were swinging
 934 pendulums with different eigenfrequencies [8,37,46].
- 935 • Transitions are also found in trajectory formation, for
 936 instance when subjects move their index finger such
 937 that they draw an “8” and this movement is sped up
 938 the pattern switches to a “0” [3,4,9].

Future Directions 939

940 One of the most exciting applications of movement co-
 941 ordination and its spontaneous transitions in particular
 942 is that they open a new window for probing the hu-
 943 man brain, made possible by the rapid development of
 944 brain-imaging technologies that allow for the recording
 945 of brain activity in a noninvasive way. Electroencephalog-

CE3 Is this correct or did you mean "patterning"?

Editor's or typesetter's annotations (will be removed before the final T_X run)

946 raphy (EEG), magnetoencephalography (MEG) and func-
 947 tional magnetic resonance tomography (fMRI) have been
 948 used in coordination experiments since the 1990s to study
 949 the changes in brain activations accompanying (or trig-
 950 gering?) the switches in movement behavior [13,33,34].
 951 Results from MEG experiments reveal a strong frequency
 952 dependence of the dominating pattern with the contri-
 953 bution of the auditory system being strongest at low
 954 metronome/movement rates, whereas at high rates the
 955 signals from sensorimotor cortex dominate [15,35]. The
 956 crossover point is found at rates around 2 Hz, right where
 957 the transitions typically take place.

958 In two other studies the rate dependence of the audi-
 959 tory and sensorimotor system was investigated separately.
 960 In an MEG experiment Carver et al. [7] found a resonance-
 961 like enhancement of a brain response that occurs about
 962 50 ms after a tone is delivered, again at a rate of about 2 Hz.
 963 In the sensorimotor system a nonlinear effect of rate was
 964 shown as well. Using a continuation paradigm, where sub-
 965 jects moved an index finger paced by a metronome which
 966 was turned off at a certain time while the subjects were
 967 to continue moving at the same rate, Mayville et al. [36]
 968 showed that a certain pattern of brain activation drops
 969 out when the movement rate exceeds about 1.5 Hz. Even
 970 though their contribution to behavioral transitions is far
 971 from being completely understood, it is clear that such
 972 nonlinear effects of rate exist in both the auditory and the
 973 sensorimotor system in parameter regions where behav-
 974 ioral transitions are observed.

975 Using fMRI brain areas have been identified that show
 976 a dependence of their activation level as a function of rate
 977 only, independent of coordination mode, whereas activa-
 978 tion in other areas strongly depends on whether subjects
 979 are syncopating or synchronizing regardless of how fast
 980 they are moving [20].

981 Taken together, these applications of coordination dy-
 982 namics to brain research have hardly scratched the sur-
 983 face so far but the results are already very exciting as
 984 they demonstrate that the experimental paradigms from
 985 movement coordination may be used to prepare the brain
 986 into a certain state where its responses can be studied.
 987 With further improvement of the imaging technologies
 988 and analysis procedures many more results can be ex-
 989 pected to contribute significantly to our understanding of
 990 how the human brain works.

991 Acknowledgment

992 Work reported herein was supported by NINDS grant
 993 48299 and NIMH grant 42900 to J.A.S.K.

Bibliography

994

Primary Literature

1. Assisi CG, Jirsa VK, Kelso JAS (2005) Dynamics of multifre-
quency coordination using parametric driving: Theory and Ex-
periment. *Biol Cybern* 93:6–21
2. Buchanan JJ, Kelso JAS (1993) Posturally induced transitions
in rhythmic multijoint limb movements. *Exp Brain Res* 94:131–
142
3. Buchanan JJ, Kelso JAS, Fuchs A (1996) Coordination dynamics
of trajectory formation. *Biol Cybern* 74:41–54
4. Buchanan JJ, Kelso JAS, DeGuzman GC (1997) The self-orga-
nization of trajectory formation: I. Experimental evidence. *Biol
Cybern* 76:257–273
5. Carson RG, Goodman D, Kelso JAS, Elliott D (1995) Phase tran-
sitions and critical fluctuations in rhythmic coordination of ip-
silateral hand and foot. *J Mot Behav* 27:211–224
6. Carson RG, Rick S, Smethurst CJ, Lison JF, Biblow WD (2000)
Neuromuscular-skeletal constraints upon the dynamics of uni-
manual and bimanual coordination. *Exp Brain Res* 131:196–
214
7. Carver FW, Fuchs A, Jantzen KJ, Kelso JAS (2002) Spatiotem-
poral Analysis of Neuromagnetic Activity Associated with Rhyth-
mic Auditory Stimulation. *Clin Neurophysiol* 113:1909–1920
8. Collins DR, Sternad D, Turvey MT (1996) An experimental note
on defining frequency competition in intersegmental coordi-
nation dynamics. *J Mot Behav* 28:299–303
9. DeGuzman GC, Kelso JAS, Buchanan JJ (1997) The self-orga-
nization of trajectory formation: II. Theoretical model. *Biol Cy-
bern* 76:275–284
10. Fink P, Kelso JAS, Jirsa VK, Foo P (2000) Local and global stabi-
lization of coordination by sensory information. *Exp Brain Res*
134:9–20
11. Fuchs A, Jirsa VK (2000) The HKB model revisited: How vary-
ing the degree of symmetry controls dynamics. *Hum Mov Sci*
19:425–449
12. Fuchs A, Kelso JAS (1994) A theoretical note on models of
Interlimb coordination. *J Exp Psychol Hum Percept Perform*
20:1088–1097
13. Fuchs A, Kelso JAS, Haken H (1992) Phase transitions in the hu-
man brain: Spatial mode dynamics. *Int J Bifurc Chaos* 2:917–
939
14. Fuchs A, Jirsa VK, Haken H, Kelso JAS (1996) Extending the HKB-
Model of coordinated movement to oscillators with different
eigenfrequencies. *Biol Cybern* 74:21–30
15. Fuchs A, Mayville JM, Cheyne D, Weinberg H, Deecke L, Kelso
JAS (2000) Spatiotemporal Analysis of Neuromagnetic Events
Underlying the Emergence of Coordinative Instabilities. *Neu-
rolmage* 12:71–84
16. Gardiner CW (1985) *Handbook of stochastic Systems*. Springer,
Heidelberg
17. Haken H (1977) *Synergetics, an introduction*. Springer, Heidel-
berg
18. Haken H (1983) *Advanced Synergetics*. Springer, Heidelberg
19. Haken H, Kelso JAS, Buz H (1985) A theoretical model of phase
transition in human movements. *Biol Cybern* 51:347–356
20. Jantzen KJ, Kelso JAS (2007) Neural coordination dynamics of
human sensorimotor behavior: A review. In: Jirsa VK, McIntosh
AR (eds) *Handbook of Brain Connectivity*. Springer, Heidelberg
21. Jeka JJ, Kelso JAS (1995) Manipulating symmetry in human



- 1053 two-limb coordination dynamics. *J Exp Psychol Hum Percept Perform* 21:360–374 1114
- 1054
- 1055 22. Jeka JJ, Kelso JAS, Kiemel T (1993) Pattern switching in human 1115
- 1056 multilimb coordination dynamics. *Bull Math Biol* 55:829–845 1116
- 1057 23. Jeka JJ, Kelso JAS, Kiemel T (1993) Spontaneous transitions and 1117
- 1058 symmetry: Pattern dynamics in human four limb coordination. 1118
- 1059 *Hum Mov Sci* 12:627–651 1119
- 1060 24. Jirsa VK, Fink P, Foo P, Kelso JAS (2000) Parameteric stabiliza- 1120
- 1061 tion of biological coordination: a theoretical model. *J Biol Phys* 1121
- 1062 26:85–112 1122
- 1063 25. Kay BA, Kelso JAS, Saltzman EL, Schöner G (1987) Space-time 1123
- 1064 behavior of single and bimanual rhythmic movements: Data 1124
- 1065 and limit cycle model. *J Exp Psychol Hum Percept Perform* 1125
- 1066 13:178–192 1126
- 1067 26. Kay BA, Saltzman EL, Kelso JAS (1991) Steady state and per- 1127
- 1068 turbed rhythmic movements: Dynamical modeling using 1128
- 1069 a variety of analytic tools. *J Exp Psychol Hum Percept Perform* 1129
- 1070 17:183–197 1130
- 1071 27. Kelso JAS (1981) On the oscillatory basis of movement. *Bull* 1131
- 1072 *Psychon Soc* 18:63 1132
- 1073 28. Kelso JAS (1984) Phase transitions and critical behavior in hu- 1133
- 1074 man bimanual coordination. *Am J Physiol Regul Integr Comp* 1134
- 1075 15:R1000–R1004 1135
- 1076 29. Kelso JAS, Jeka JJ (1992) Symmetry breaking dynamics of hu- 1136
- 1077 man multilimb coordination. *J Exp Psychol Hum Percept Per-* 1137
- 1078 *form* 18:645–668 1138
- 1079 30. Kelso JAS, Scholz JP, Schöner G (1986) Nonequilibrium phase 1139
- 1080 transitions in coordinated biological motion: Critical fluctua- 1140
- 1081 tions. *Phys Lett A* 118:279–284 1141
- 1082 31. Kelso JAS, Schöner G, Scholz JP, Haken H (1987) Phase locked 1142
- 1083 modes, phase transitions and component oscillators in coordi- 1143
- 1084 nated biological motion. *Phys Scr* 35:79–87 1144
- 1085 32. Kelso JAS, DelColle J, Schöner G (1990) Action-perception as 1145
- 1086 a pattern forming process. In: Jannerod M (ed) *Attention and* 1146
- 1087 *performance XIII*. Erlbaum, Hillsdale, pp 139–169
- 1088 33. Kelso JAS, Bressler SL, Buchanan S, DeGuzman GC, Ding M, 1147
- 1089 Fuchs A, Holroyd T (1992) A phase transition in human brain 1148
- 1090 and behavior. *Phys Lett A* 169:134–144 1149
- 1091 34. Kelso JAS, Fuchs A, Holroyd T, Lancaster R, Cheyne D, Weinberg 1150
- 1092 H (1998) Dynamic cortical activity in the human brain reveals 1151
- 1093 motor equivalence. *Nature* 392:814–818 1152
- 1094 35. Mayville JM, Fuchs A, Ding M, Cheyne D, Deecke L, Kelso JAS 1153
- 1095 (2001) Event-related changes in neuromagnetic activity associ- 1154
- 1096 ated with syncope and synchronization timing tasks. *Hum* 1155
- 1097 *Brain Mapp* 14:65–80 1156
- 1098 36. Mayville JM, Fuchs A, Kelso JAS (2005) Neuromagnetic Motor 1157
- 1099 Fields Accompanying Self-paced Rhythmic Finger Movements 1158
- 1100 of Different Rates. *Exp Brain Res* 166:190–199 1159
- 1101 37. Park H, Turvey MT (2008) Imperfect symmetry and the elemen- 1160
- 1102 tary coordination law. In: Fuchs A, Jirsa VK (eds) *Coordination:* 1161
- 1103 *Neural, Behavioral and Social Dynamics*. Springer, Heidelberg, 1162
- 1104 pp 3–25 1163
- 1105 38. Peper CE, Beek PJ (1998) Distinguishing between the effects 1164
- 1106 of frequency and amplitude on interlimb coupling in tapping 1165
- 1107 a 2:3 polyrhythm. *Exp Brain Res* 118:78–92 1166
- 1108 39. Peper CE, Beek PJ, van Wieringen PC (1995) Frequency-in- 1167
- 1109 duced phase transitions in bimanual tapping. *Biol Cybern* 1168
- 1110 73:303–309 1169
- 1111 40. Post AA, Peeper CE, Daffertshofer A, Beek PJ (2000) Relative 1170
- 1112 phase dynamics in perturbed interlimb coordination: stability 1171
- 1113 and stochasticity. *Biol Cybern* 83:443–459 1172
41. Schmidt RC, Beek PJ, Treffner PJ, Turvey MT (1991) Dynamical 1173
- substructure of coordinated rhythmic movements. *J Exp Psy-* 1174
- chol Hum Percept Perform* 17:635–651 1175
42. Schöner G, Kelso JAS (1988) Dynamic pattern generation in be- 1176
- havioral and neural systems. *Science* 239:1513–1520 1177
43. Schöner G, Haken H, Kelso JAS (1986) A stochastic theory of 1178
- phase transitions in human hand movements. *Biol Cybern* 1179
- 53:442–453 1180
44. Scholz JP, Kelso JAS (1989) A quantitative approach to under- 1181
- standing the formation and change of coordinated movement 1182
- patterns. *J Mot Behav* 21:122–144 1183
45. Scholz JP, Kelso JAS, Schöner G (1987) Nonequilibrium phase 1184
- transitions in coordinated biological motion: Critical slowing 1185
- down and switching time. *Phys Lett A* 8:90–394 1186
46. Sternad D, Collins D, Turvey MT (1995) The detuning factor in 1187
- the dynamics of interlimb rhythmic coordination. *Biol Cybern* 1188
- 73:27–35 1189
47. Sternad D, Turvey MT, Saltzman EL (1999) Dynamics of 1:2 Co- 1190
- ordination: Generalizing Relative Phase to n:m Rhythms. *J Mot* 1191
- Behav* 31:207–233 1192
- Books and Reviews** 1193
- Fuchs A, Jirsa VK (eds) (2007) *Coordination: Neural, Behavioral and* 1194
- Social Dynamics*. Springer, Heidelberg 1195
- Jirsa VK, Kelso JAS (eds) (2004) *Coordination Dynamics: Issues and* 1196
- Trends*. Springer, Heidelberg 1197
- Kelso JAS (1995) *Dynamics Patterns: The Self-Organization of Brain* 1198
- and Behavior*. MIT Press, Cambridge 1199
- Haken H (1996) *Principles of Brain Functioning*. Springer, Heidel- 1200
- berg 1201
- Tschacher W, Dauwalder JP (eds) (2003) *The Dynamical Systems* 1202
- Approach to Cognition: Concepts and Empirical Paradigms* 1203
- Based on Self-Organization, Embodiment and Coordination* 1204
- Dynamics*. World Scientific, Singapore 1205

Uncorrected Proof
2008-08-22